

Jun Yan, Brian M. Barnes, Franziska Kohl and Thomas G. Marr

Physiol Genomics 32:170-181, 2008. First published Oct 9, 2007;

doi:10.1152/physiolgenomics.00075.2007

You might find this additional information useful...

Supplemental material for this article can be found at:

<http://physiolgenomics.physiology.org/cgi/content/full/00075.2007/DC1>

This article cites 58 articles, 36 of which you can access free at:

<http://physiolgenomics.physiology.org/cgi/content/full/32/2/170#BIBL>

Updated information and services including high-resolution figures, can be found at:

<http://physiolgenomics.physiology.org/cgi/content/full/32/2/170>

Additional material and information about *Physiological Genomics* can be found at:

<http://www.the-aps.org/publications/pg>

This information is current as of January 18, 2008 .

Modulation of gene expression in hibernating arctic ground squirrels

Jun Yan,^{1,2} Brian M. Barnes,¹ Franziska Kohl,¹ and Thomas G. Marr^{1,3}

¹Institute of Arctic Biology, University of Alaska Fairbanks, Fairbanks, Alaska; ²CAS-MPG Partner Institute for Computational Biology, Shanghai Institutes of Biological Sciences, Shanghai, China; and ³Hiberna Corporation, Boulder, Colorado

Submitted 31 March 2007; accepted in final form 27 September 2007

Yan J, Barnes BM, Kohl F, Marr TG. Modulation of gene expression in hibernating arctic ground squirrels. *Physiol Genomics* 32: 170–181, 2008. First published October 9, 2007; doi:10.1152/physiolgenomics.00075.2007.—We performed a broad-scale screening of differential gene expression using both high-throughput bead-array technology and real-time PCR assay in brown adipose tissue, liver, heart, hypothalamus, and skeletal muscle in hibernating arctic ground squirrels, comparing animals sampled after two durations of steady-state torpor, during two stages of spontaneous arousal episodes, and in animals after they ended hibernation. Significant seasonal and torpor-arousal cycle differences of gene expression were detected in genes involved in glycolysis, fatty acid metabolism, gluconeogenesis, amino acid metabolism, molecular transport, detoxification, cardiac contractility, circadian rhythm, cell growth and apoptosis, muscle dystrophy, and RNA and protein protection. We observed, for the first time, complex modulation of gene expression during multiple stages of torpor-arousal cycles. The mRNA levels of certain metabolic genes drop significantly during the transition from late torpor to early arousal, perhaps due to the rapid turnover of mRNA transcripts resulting from the translational demands during thermogenesis in early arousal, whereas the mRNA levels of genes related to circadian rhythm, cell growth, and apoptosis rise significantly in the early or late arousal phases during torpor-arousal cycle, suggesting the resumption of circadian rhythm and cell cycle during arousal.

metabolism; cardiac contractility; circadian rhythm; muscle dystrophy; cell cycle

MAMMALIAN HIBERNATORS ACHIEVE profound energy savings and enter a stasis that can include protection from trauma by a regulated suppression of metabolic rate and tolerance of low body temperatures (9, 20, 29). Hibernators from highly seasonal environments anticipate decreases in food availability by fattening and/or caching food and retreating to protected hibernacula. They have evolved remarkable abilities to sustain suppressed levels of respiratory, cardiovascular, immunological, neurological, and metabolic rates and functions that would be life-threatening in other mammals.

The arctic ground squirrel (*Spermophilus parryii*) is an exceptional species for the study of hibernation. During the 6- to 9-mo-long hibernation season, arctic ground squirrels enter torpor by lowering core body temperatures to as low as -2.9°C and metabolic rates to 1–2% of basal metabolism (3, 12). However, in regular arousal episodes they spontaneously rewarm to euthermic levels ($36\text{--}37^{\circ}\text{C}$) every 10–21 days and maintain that temperature for 15–24 h before reentering torpor.

All small mammalian hibernators exhibit these periodic arousals from torpor in spite of the significant energetic cost of rewarming. The functional significance of arousal episodes is unknown, but their universal occurrence in small hibernators suggests a limit to how long deep states of hypothermia and hypometabolism can persist in mammals. Recent theories of the functional need for arousal episodes include that hibernators rewarm to achieve sleep (5, 19, 30, 53), to replenish gene products (38), or for immune responsiveness (46). Describing molecular processes during the torpor-arousal cycle in hibernators may provide insight into the function of arousal episodes.

It is hypothesized that the ability to prepare for, enter, and reverse hibernation is a pleiomorphic trait that is regulated by the differential expression of common mammalian genes, rather than the result of independent evolution of derived genes (9, 15, 36, 51). Recent broad-scale gene expression studies on several hibernating rodent species have provided evidence that differences in gene expression occur on the mRNA level in a tissue-specific manner during hibernation. Brauch et al. (10) generated a cDNA library covering 3,532 genes for the heart in thirteen-line ground squirrels (*Spermophilus tridecemlineatus*) and identified differential expression of 48 genes by comparing the mRNA profiles in heart tissue sampled from winter-torpid vs. summer-active ground squirrels. Using microarrays generated from a cDNA library for the golden-mantled ground squirrel (*Spermophilus lateralis*) covering over 5,100 genes, Williams et al. (58) identified differential expression between winter-torpid and summer-active ground squirrels in 102 cDNAs in liver, 115 cDNAs in heart, and 78 cDNAs in brain, respectively. Although they included animals sampled after arousal in their study, they did not find any significant differential gene expression during torpor-arousal cycles in those three tissues. In a previous study using broad-scale mouse microarrays, we identified the differential expression of 625 genes in brown adipose tissue (BAT), comparing winter-torpid with summer-active arctic ground squirrels (59). Genes involved in nonshivering thermogenesis (NST) were significantly overexpressed, whereas those involved in protein synthesis were significantly underexpressed in winter-torpid animals compared with summer-active animals. However, the use of a heterologous assay is problematic as mouse (*Mus musculus*) only shares on average 89% mRNA sequence identities with the arctic ground squirrel. Although the mouse microarray study generated a large number of candidate genes involved in regulation and tolerance of hibernation, it may also have increased false positive and negative errors due to nonspecific hybridization to heterologous cDNA probes. In this study, we use a new high-throughput gene expression profiling technology: Illumina bead array.

Article published online before print. See web site for date of publication (<http://physiolgenomics.physiology.org>).

Address for reprint requests and other correspondence: J. Yan, CAS-MPG Partner Inst. for Computational Biology, Shanghai Institutes of Biological Sciences, 320 Yue Yang Rd., Shanghai, 200031, China (e-mail: junyan@picb.ac.cn).

MATERIALS AND METHODS

Animals. Adult arctic ground squirrels (*S. parryii kennicottii*) were trapped during July on the North Slope of Alaska near Toolik Lake (68°N 149°W, elevation 809 m) and transported to University of Alaska Fairbanks. Animals were housed at $18 \pm 2^\circ\text{C}$ with a 16-h light:8-h dark (16L:8D) photoperiod and provided with Mazuri Rodent Chow and water ad libitum, with supplements of sunflower seeds, carrots, and apple slices. Animals were transferred in September to a room at $5 \pm 1^\circ\text{C}$ with a photoperiod of 4L:20D where they entered hibernation; all animals remained in these conditions for the remainder of the experiment. Food and water remained available to animals during hibernation although there was no evidence that any was consumed. A pilot study using a 16-sample bead chip compared animals in torpor (T, $n = 9$) with nonhibernating animals following seasonal reproductive maturation [postreproduction (PR), $n = 7$]. Animals in torpor in the pilot study were monitored by the traditional sawdust method, i.e., wood shavings were placed on the dorsal surface of the animals and inspected twice daily to assess by their presence or absence the duration of torpor bouts and occurrence of arousal episodes. Tissues were collected from animals in torpor after no fewer than 5 days of continuous torpor in at least the third torpor bout of the winter hibernation season. For nonhibernating controls, tissues were collected from animals that were at euthermic body temperatures after spontaneously ending hibernation, completing reproductive maturation and regression as assessed by external inspection of gonads and genitalia (4, 11), and entering molt. Hibernating animals used in the 96-sample array matrix experiment were housed at $5 \pm 1^\circ\text{C}$ with a 4L:20D photoperiod and monitored for precise stages of torpor and arousal by an automated telemetry system that recorded core body temperatures (T_b) every 10 min, as indicated by temperature-sensitive transmitters implanted in abdomens of animals during the previous summer (12). Animals were sampled in four states of hibernation: early in a torpor bout, after 10–20% of the duration of the previous torpor bout [early torpor (ET), $n = 4$]; late in a torpor bout, after 80–90% of the duration of the previous torpor bout [late torpor (LT), $n = 5$]; early after spontaneous arousal, 1–2 h after T_b had increased $>30^\circ\text{C}$ during rewarming [early arousal (EA), $n = 4$]; and later in the arousal episode, 7–8 h after T_b had increased $>30^\circ\text{C}$ [late arousal (LA), $n = 4$]. These four states of hibernation in a telemetered animal are illustrated in Fig. 1. For the real-time PCR assay, we added eight more animals (two more for hypothalamus) with transmitters to the 24 animals used in the array matrix experiment. A total of 32 (26 for hypothalamus) animals including EA ($n = 6$; $n = 5$ for hypothalamus), LA ($n = 7$; $n = 5$ for hypothalamus), ET ($n = 4$), LT ($n = 7$;

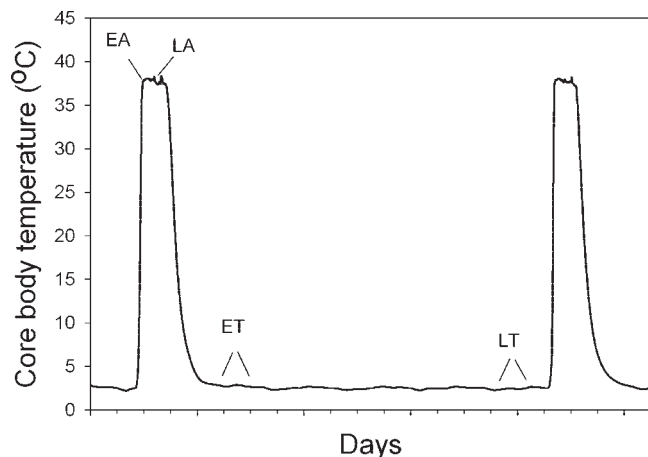


Fig. 1. The 4 stages in the torpor-arousal cycle, early arousal (EA), late arousal (LA), early torpor (ET), late torpor (LT), during hibernation in a telemetered animal.

$n = 5$ for hypothalamus), and postreproductive animals (PR, $n = 8$; $n = 7$ for hypothalamus) were used in the real-time PCR assay. Animals sampled during arousal episodes had T_b of $35\text{--}37^\circ\text{C}$, and animals sampled during torpor had T_b of $5\text{--}7^\circ\text{C}$. Animals in torpor were euthanized by decapitation without anesthesia. Animals in arousal and postreproduction were deeply anesthetized by exposure to 5% isoflurane for 5–8 min before decapitation. BAT, liver, heart, hypothalamus, and skeletal muscle were rapidly dissected, frozen in liquid nitrogen, and stored at -80°C until total RNA was isolated at a later date. Animal protocols were approved by the University of Alaska Fairbanks Institutional Animal Care and Use Committee.

Illumina bead array. Illumina bead-array gene expression profiling technology uses pooled libraries of $3\ \mu\text{m}$ beads, each covalently attached with $>10^5$ copies of identical oligonucleotide probes (34). The beads self-assemble into the etched wells on the surface of an array with one bead per well. Each bead array can support 50,000 beads representing 1,500 unique probes with 30-fold redundancy for each probe. Each oligonucleotide probe is concatenated by a 23-mer address sequence used to determine the location of the probe on the bead array during the decoding process (27). A 50-mer gene-specific sequence is used to hybridize with the fluorescently labeled RNA sequences. Seven hundred genes can be represented on a customized bead array with two probes designed for each gene. As a result of the high redundancy built in the bead array, it has exhibited high selectivity and sensitivity in gene expression profiling (34). We customized two formats of bead array named 1A and 2A covering 1,407 genes in total with probes designed from available ground squirrel mRNA sequences. Two types of high-throughput bead-array platforms were used in this study: 16-sample bead chip and 96-sample array matrix. The high-throughput design of these two bead-array platforms enabled us to include a wide range of tissues (BAT, liver, heart, hypothalamus, and skeletal muscle) and compare multiple stages (EA, LA, ET, and LT) during hibernation with animals sampled after the end of hibernation in our study.

Sample preparation and hybridization. Total RNA was prepared from frozen tissues by homogenizing directly in liquid nitrogen using RNeasy kit (Qiagen) with mortar and pestle. Tissues from heart and skeletal muscle were treated by proteinase K digestion to remove connective tissues prior to RNA extraction. RNA was processed by DNase I treatment, and RNA quality was assessed by 1.2% formaldehyde agarose gel electrophoresis under the denaturing condition using ethidium bromide poststaining. The density of total RNA of each sample was measured by a spectrophotometer. We subsequently linearly amplified 100 ng of each total RNA sample with an Ambion Illumina RNA Amplification kit (Ambion) using a modified T7 Eberwine procedure (54). Biotin-16-UTP (Enzo) was used during the in vitro transcription. All samples of the same tissue were amplified in the same batch. Labeled amplified RNA ($1\ \mu\text{g}$ per array on 96-sample array matrix and 500 ng per array on 16-sample bead chip) was hybridized onto each array and incubated at 55°C for 16 h followed by washing and blocking steps according to the manufacturer's instructions. Streptavidin-Cy3 (Amersham Biosciences) was used to cross-link Cy3 with biotin labeled amplified RNA. The arrays were scanned by an Illumina Bead Array Reader scanner according to manufacturer's instructions. Array data were processed and analyzed by Illumina BeadStudio software.

Bead-array probe design. Bead-array probes were designed from nonredundant high-quality cDNA sequences of three closely related ground squirrel species: *S. lateralis*, *S. parryii*, and *S. tridecemlineatus*. *S. lateralis* and *S. tridecemlineatus* share on average 99% mRNA sequence identities with *S. parryii* at the nucleotide level (59). *S. lateralis* sequences were downloaded from squirrelBASE 2.0 (Nov. 10, 2003) of Laboratory for Environmental Gene Regulation (LEGR) Data Centre at Liverpool University (<http://legr.liv.ac.uk>). Among 5,109 subgroups [expressed sequence tag (EST) clusters] in squirrelBASE 2.0, only the 1,846 subgroups aligned with SwissProt were used in this study. We also downloaded the annotation and

alignment information for the SwissProt aligned subgroups. To guarantee the quality and nonredundancy of the sequences, we further processed them according to the following procedures: 1) Sequences outside the SwissProt alignments were trimmed to avoid vector contamination and sequencing errors. 2) If more than one subgroup belonged to the same group (EST clusters with a less stringent condition), we only kept the subgroup with the longest SwissProt alignment in that group. 3) All sequences were repeat-masked by RepeatMasker (50), and sequences with unmasked nucleotides <150 bp were removed. 4) The sequences annotated as hypothetical proteins were removed. 5) Reverse complements were used for the sequences aligned in the reverse complement direction. After this preliminary processing, 1,545 *S. lateralis* sequences remained. Among these, 1,329 sequences were actually used in the bead-array probe design; 81 *S. parryii* genes (GenBank accessions: DQ333962–DQ334051) were previously sequenced (59). These *S. parryii* sequences were aligned against the *S. lateralis* sequences using the blastn program (1) to identify those that already existed in the *S. lateralis* sequences. After removing redundant sequences, we obtained 62 *S. parryii* sequences suitable for the probe design. In addition, 16 nonredundant *S. tridecemlineatus* sequences downloaded from GenBank were also used in the probe design. Seven genes: actin beta (*Actb*), eukaryotic translation elongation factor 1 alpha 1 (*Eef1a1*), glyceraldehyde-3-phosphate dehydrogenase (*Gapd*), ribosomal protein S9 (*Rps9*), tubulin beta 2B (*Tubb2b*), ribosomal protein S3 (*Rps3*), and ubiquitin C (*Ubc*) were chosen as housekeeping genes to be present on both 1A and 2A arrays. They were used as controls for hybridization between our ground squirrel probes and labeled AGS (arctic ground squirrel) cRNA. The choice of housekeeping genes does not affect the downstream analysis. Overall, 1,407 ground squirrel sequences were sent to Illumina for the probe design. Two 50 bps probes were designed for every gene except for three genes on 2A array: heat shock 10 kDa protein 1 (*Hspe1*); major histocompatibility complex, class II, DP beta 1 (*Hla-dpb1*); and 1-acylglycerol-3-phosphate O-acyltransferase 3 (*Acpat3*) with only one 50 bp probe designed. The sequence sources of the genes on 1A and 2A arrays are shown in Table 1. To obtain standard gene names and symbols for the 1,407 ground squirrel sequences, we aligned them onto the RefSeq (47) sequences using the blastn program (1). The RefSeq sequence with the highest blast score was identified to be the homologous sequence for each ground squirrel sequence. The accession numbers of homologous RefSeq sequences were then uploaded to Stanford Source (<http://source.stanford.edu>) to obtain the gene names and symbols.

Data analysis. The array data were background subtracted and normalized using the rank-invariant method in the Illumina BeadStudio software. The detection score (detection probability between 0 and 1) of each gene on every array was also obtained using the Illumina BeadStudio software. For the 16-sample bead-chip experiment, a two-stage analysis comparing torpor (T) with PR was done. For the 96-sample array matrix experiment, a three-stage analysis among arousal (A), T, and PR was done where A = EA + LA and T = ET + LT. The detection score of each gene in any stage (T and PR in the two-stage analysis and A, T, PR in the three-stage analysis) is defined as the median value of detection scores of all arrays in that stage. The detection score of a gene is defined as the maximum value of detection

Table 1. Sequence sources of the genes on 1A and 2A arrays

Sequence Sources	1A Array	2A Array	Housekeeping Genes	Total
<i>Spermophilus lateralis</i>	628	700	1	1,329
<i>Spermophilus parryii</i>	60	0	2	62
<i>Spermophilus tridecemlineatus</i>	12	0	4	16

The sequence sources of the genes on 1A and 2A arrays. Each array 700 genes in addition to the 7 housekeeping genes.

scores of all stages included in the analysis. We only included the genes with a detection score >0.99 in the analyses. This definition of the detection score allowed us to include genes only detected in one particular stage but not other stages in our analyses. In the two-stage analysis (T vs. PR), Welch two-sample *t*-test was used. In the three-stage analysis (A, T, PR), one-way ANOVA followed by post hoc Tukey's test with honestly significant difference was used. $P < 0.05$ was used as the criterion for statistical significance. All statistical analyses were done in R. All microarray data series were submitted to National Center for Biotechnology Information Gene Expression Omnibus with accession number: GSE5414.

Real-time PCR. We conducted a total of 495 real-time PCR tests including 300 tests on the differentially expressed genes identified in the three-stage analysis in 96-sample array matrix experiments and in the two-stage analysis in 16-sample bead-chip experiments. We also tested an additional 39 genes involved in circadian rhythm and cell growth and apoptosis by real-time PCR in all five tissues; these include circadian rhythm (*Per1*, *Per3*, *Bmal1*, *Cry1*, *Cry2*, *Timeless*, *Clock*, *Bhlhb2*); MAP kinase pathway (*Mapk1*, *Mapk3*, *Mapk14*, *Map2k1*, *Map3k1*, *Map3k5*, *Raf1*, *Map4k3*); immediate early genes (*c-myc*, *c-fos*, *c-jun*); Bcl2 family (*Bcl2*, *Bcl2l1-xL*, *Bax*, *Bid*); tumor suppressor gene (*P53*); caspases (*Casp3*, *Casp6*); TGF β pathway (*Tgfb1*, *Tgfb2*, *Tgfb1i4*, *Tgfbri1*); and others (*E2f6*, *Birc2*, *Rac1*, *Src*, *Nfkb1*, *Pik3r1*, *Hif1a*, *Igf1r*, *Foxo1a*). Gene-specific primers were designed based on the ground squirrel sequences pooled from *S. lateralis*, *S. parryii*, and *S. tridecemlineatus* using Primer Express software (Applied Biosystem). The sequences of primer pairs are listed in Table S1 (supplementary materials).¹ Two-step real-time PCR was performed on an ABI-7900 HT system (Applied Biosystem) using SYBR Green reagent (Applied Biosystem). The density of total RNA of each sample was measured by a spectrophotometer. The cDNA was synthesized from 100 ng total RNA of each sample using Multiscribe reverse transcriptase (Applied Biosystem) with random hexamer primer in a 10 μ l reaction at 25°C for 10 min, 48°C for 30 min, and 95°C for 5 min. The synthesized cDNA was 10 \times diluted using RNase-free water into a 100 μ l solution. We used 4 μ l of diluted cDNA solution in each 20 μ l real-time PCR reaction. Cycle parameters were: 95°C for 10 min hot start and 40 cycles of 95°C for 15s; and 60°C for 1 min. The 18S gene (GenBank accession: X00686) was used as an endogenous housekeeping gene for normalization. PCR product specificity was checked by melting curve analysis. The critical threshold (C_T) value is the PCR cycle number where the PCR growth curve crosses a defined threshold in the linear range of the reaction. C_T can be related to gene expression values by $\log_2(\text{expression value}) = -\Delta C_T$, where ΔC_T is the difference between the critical threshold of the target gene and that of the 18S gene.

Similar to the data analyses on the bead arrays, one-way ANOVA followed by post hoc Tukey's test was used on $-\Delta C_T$ in three-stage (A, T, PR) analysis. In addition, a four-stage analysis among EA, LA, ET, and LT was also carried out by one-way ANOVA followed by post hoc Tukey's test. $P < 0.05$ was used as the criterion for statistical significance. To make a more direct comparison with Illumina bead-array measurements in Fig. 2, ΔC_T of each sample was subtracted by the ΔC_T of the first early arousal animal (labeled as EA1 in our experiment) to obtain $\Delta\Delta C_T$. Normalized expression values in real-time PCR were calculated as $2^{-\Delta\Delta C_T}$. The expression value on Illumina bead arrays of each sample was also divided by that of EA1 to obtain a normalized expression value. The normalized expression values calculated for both Illumina bead arrays and real-time PCR were used to plot Fig. 2. The error bars in the figures represent the SD of expression in each stage. We used TreeView software (21) to plot $-\Delta C_T$ after subtracting the median for each gene in the form of heat maps. Genes were arranged according to their functional categories and animals according to their hibernation stages. Red and green

¹ The online version of this article contains supplemental material.

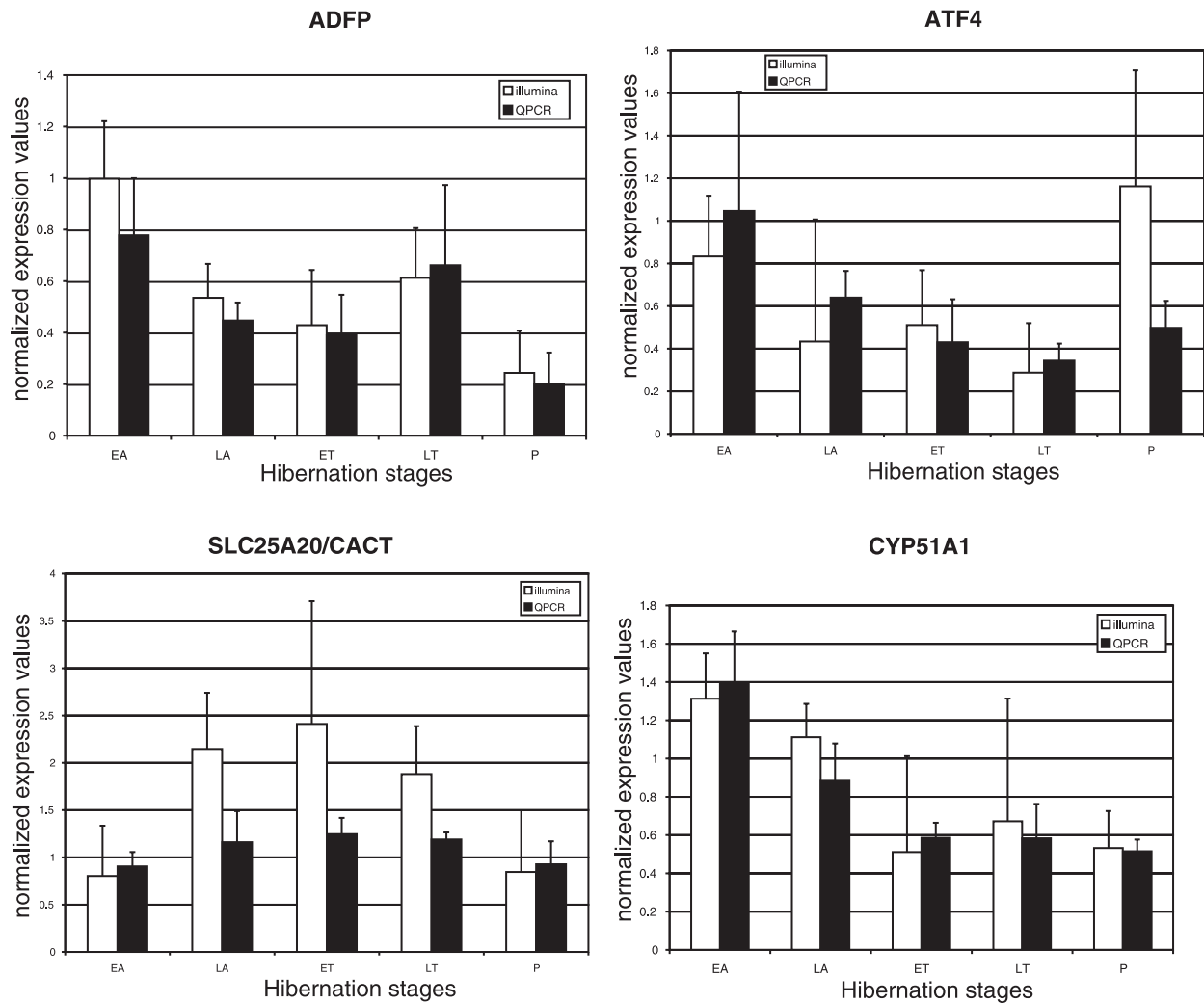


Fig. 2. Four genes with significant modulation of expression during torpor-arousal cycle of hibernation. Four genes: *Adfp* in brown adipose tissue (BAT, top left), *Atf4* in liver (top right), *Cacu/Slc25a20* in heart (bottom left), and *Cyp51a1* in hypothalamus (bottom right) during EA, LA, ET, LT, and postreproduction (P) as measured by both Illumina bead arrays and real-time PCR (QPCR). Error bars in the figure are SDs. All of them showed significant ($P < 0.05$) modulation in 4-stage analysis during torpor-arousal cycles in real-time PCR (Table S5). The method to calculate the normalized gene expression values is given in MATERIALS AND METHODS.

colors represent high and low levels of gene expression, respectively, in \log_2 scale. The heat map in liver is shown in Fig. 3, and heat maps in other tissues are included in the supplemental materials.

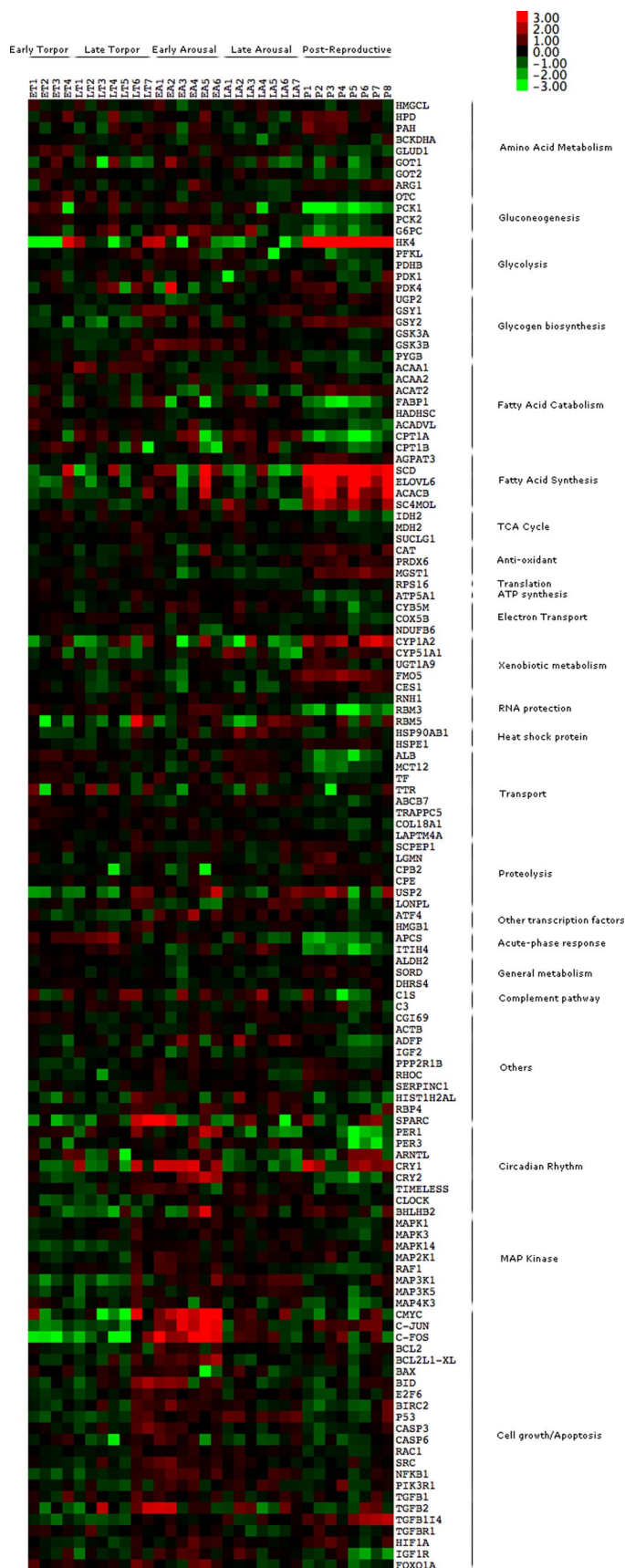
RESULTS

As a pilot study, BAT, liver, and skeletal muscle from animals in T during the hibernation season and PR (nonhibernating controls) were assayed on six Illumina 16-sample bead chips. Using a stringent detection criterion, we detected 317 out of 1,407 genes in at least one tissue. Two-stage analysis between torpor and PR was carried out by Welch's *t*-test. Among the three tissues, liver showed the most detected and differentially expressed genes. The complete lists of detected and differentially expressed ($P < 0.05$) genes are in Table S2a, S2b, and S2c.

In a second experiment, BAT, liver, heart, and hypothalamus of 24 arctic ground squirrels sampled early and late in a torpor bout and early and late in a spontaneous arousal episode together with PR animals were assayed on two Illumina 96-sample Array Matrices. To compare two Illumina bead-array

platforms (96-sample array matrix and 16-sample bead chip), we also carried out two-stage analysis between torpor (ET and LT combined, i.e., T = ET + LT) and PR for BAT and liver on 96-sample array matrices. We compared the BAT and liver results on 96-sample array matrices with those on 16-sample bead chips. Of the genes identified as significantly different in the 16-sample bead-chip experiment, 20 of 46 in BAT and 28 of 62 in liver were again significantly different in the 96-sample array matrices. All of these genes showed consistent over- or underexpression between the two platforms except insulin-like growth factor 2 (*Igf2*) in liver, which is underexpressed in the 16-sample bead-chip experiment but overexpressed in the 96-sample array matrix experiment. This indicates that our results are generally consistent and repeatable in separate experiments.

A three-stage analysis between animals sampled during an arousal episode (EA and LA combined, i.e., A = EA + LA), torpor (ET and LT combined), and PR in BAT, liver, heart, and hypothalamus, respectively, on 96-sample array matrices was



carried out with one-way ANOVA followed by post hoc Tukey's test. The complete lists of detected and differentially expressed genes ($P < 0.05$) in each tissue are given in Table S3a, S3b, S3c, and S3d, respectively.

We tested the differentially expressed genes identified in Illumina bead-array experiments together with an additional 39 genes involved in circadian rhythm and cell growth and apoptosis in all five tissues by real-time PCR assay with an enlarged sample size. The same three-stage analysis was carried out on the normalized critical threshold $-\Delta C_T$ in real-time PCR, which corresponds to the $\log_2(\text{normalized expression value})$ on bead arrays. The complete results of three-stage analysis in all tissues are shown in Table S4. General agreement between bead-array experiments and real-time PCR assay was found in all tissues. In liver, for example, 42 of 62 genes identified as differentially expressed in 96-sample array matrix experiments also showed significant ($P < 0.05$) differential expression in real-time PCR assay. Most of these genes showed consistent over- or underexpression when torpor was compared with PR, although we observed discrepancies for a few genes. For example, *Pck2* (complete gene name in Table S4) showed significant underexpression in torpor compared with PR on the 96-sample array matrix but showed significant overexpression in real-time PCR. Because other enzymes involved in gluconeogenesis in liver, including *Pck1* and *G6pc*, both showed consistent overexpression in torpor compared with PR in both bead arrays and real-time PCR assay, we concluded that *Pck2* in liver was misclassified on the beadarrays. Comparing arousal to torpor, real-time PCR generally showed fewer significant differences than bead-array results in BAT, liver, and heart but more significant differences in hypothalamus. On the bead arrays, *Alb* and *Slc16a12* (or *Mct12*) in liver were shown to be overexpressed in torpor compared with PR and underexpressed in arousal compared with torpor. Real-time PCR verified their overexpression in torpor compared with PR but failed to show their underexpression in arousal compared with torpor. Although skeletal muscle was only studied in the 16-sample bead-chip experiment and not in the 96-sample array matrix experiment, we still tested most of the differentially expressed genes identified in the 16-sample bead-chip experiment using real-time PCR on 32 samples. Excellent agreement between the results obtained with real-time PCR and the 16-sample bead-chip experiment was found when comparing torpor with PR. The expression of *Adfp* in BAT, *Atf4* in liver, *Cact* in heart, and *Cyp51a1* in hypothalamus as measured in both real-time PCR assay and Illumina bead-array experiments is shown in Fig. 2.

We represent the differential gene expression patterns in three-stage analyses by $(X_{A-T}, X_{A-PR}, X_{T-PR})$, where $X_{I-J} = 1$ if the gene expression in stage I is significantly higher than that in stage J; -1 if significantly lower; 0 if not significantly different; $I, J = A$ (arousal), T (torpor), PR (postreproduction). $P < 0.05$ in post hoc Tukey's test is used as the criterion for significance. As shown in Table 2, a total of 15 different patterns were observed. The two most abundant patterns: $(0, 1, 1)$ with 62 cases and $(0, -1, -1)$ with 41 cases correspond to

Fig. 3. Gene expression revealed in real-time PCR assay for animals at different stages and genes in different functional categories in the liver. Red and blue colors represent high and low gene expression, respectively, in \log_2 scale.

Table 2. Differential gene expression patterns in three-stage analysis

Expression Patterns	Gene Symbols
(0, 1, 1) (62 cases)	Pdk4 ^B , Acadm ^B , Cpt1a ^B , Cact ^B , Agpat3 ^B , Polr2e ^B , Rbm3 ^B , Adcy6 ^B , Adfp ^B , CGI-69 ^B , Map11c3b ^B , Glud1 ^L , Got2 ^L , Pck1 ^L , Pck2 ^L , G6pc ^L , Fabp1 ^L , Hadhsc ^L , Acadvl ^L , Cpt1a ^L , Idh2 ^L , Mdh2 ^L , Atp5a1 ^L , Rbm3 ^L , Alb ^L , Mct12 ^L , Abcb7 ^L , Col18a1 ^L , Itih4 ^L , Pygb ^L , Raf1 ^L , Foxo1a ^L , Myl6 ^{HE} , Tmed4 ^{HE} , Pdhb ^{HE} , Pdk4 ^{HE} , Cpt1a ^{HE} , Fabp3 ^{HE} , Rbm3 ^{HE} , Rnh1 ^{HE} , Ucp2 ^{HE} , CGI-69 ^{HE} , Adfp ^{HE} , Map3k5 ^{HE} , Acl3 ^{HY} , Rbm3 ^{HY} , Laptm4a ^{HY} , TF ^{HY} , Psm7 ^{HY} , Bhlhb2 ^{HY} , Tmbim4 ^{HY} , Them2 ^{HY} , Cry2 ^{HY} , c-myc ^{HY} , Pdk4 ^S , Cpt1a ^S , Rps2 ^S , Rbm3 ^S , Rnh1 ^S , Wsb2 ^S , Adfp ^S , Mapk3 ^S
(0, -1, -1) (41 cases)	Scd ^B , Prdx6 ^B , Sepp1 ^B , Arg1 ^L , Hk4 ^L , Acat2 ^L , Agpat3 ^L , Scd ^L , Elovl6 ^L , Acacab ^L , Sc4mol ^L , Cat ^L , Prdx6 ^L , Cyp1a2 ^L , Fmo5 ^L , Hspe1 ^L , Ugp2 ^L , Bckdhh ^{HE} , Hpd ^{HE} , Idh2 ^{HE} , Hsp90ab1 ^{HE} , Hba1 ^{HE} , c-jun ^{HE} , E2f6 ^{HE} , Pik3r1 ^{HE} , Lonpl ^{HY} , Map2k1 ^{HY} , Map3k5 ^{HY} , Bcl2 ^{HY} , Bax ^{HY} , E2f6 ^{HY} , Rac1 ^{HY} , Src ^{HY} , Pik3r1 ^{HY} , Tgfb1i4 ^{HY} , Hif1a ^{HY} , Pfkms ^S , Gpd1 ^S , Atf4 ^S , P53 ^S , Tgfb1i4 ^S
(0, 1, 0) (19 cases)	IDH2 ^B , Map2k1 ^B , Pdhb ^L , Hist1 h2al ^L , TF ^L , Laptm4a ^L , Per3 ^L , Mapk1 ^L , Mapk3 ^L , E2f6 ^L , Birc2 ^L , Igf1 ^L , Eif4b ^{HE} , Hk1 ^{HY} , Elovl6 ^{HY} , Srp9 ^{HY} , Cry1 ^{HY} , Map3k5 ^S , c-myc ^S
(0, 0, 1) (18 cases)	Acadvl ^B , Hadha ^B , Mdh2 ^B , Trappc5 ^L , Per1 ^L , Got2 ^{HE} , Cact ^{HE} , Cpt1b ^{HE} , Hspe1 ^{HE} , Wsb2 ^{HE} , Mapk3 ^{HE} , Bckdhh ^{HY} , Rsu1 ^{HY} , Acadm ^{HY} , Cox5b ^{HY} , Per1 ^{HY} , Cpt1b ^S , Hadhsc ^S
(0, -1, 0) (17 cases)	Fmo5 ^B , Igf2 ^B , Tgfb2 ^B , Ces1 ^L , Sord ^L , Eef1a1 ^{HE} , Alad ^{HE} , Src ^{HE} , Foxo1a ^{HE} , Hba1 ^{HY} , Map4k3 ^{HY} , Tgfb1 ^{HY} , Tgfb1 ^{HY} , Foxo1a ^{HY} , Ca3 ^S , Ckm ^S , Pkm2 ^S
(1, 1, 0) (17 cases)	Cry2 ^B , Atf4 ^L , Hsp90ab1 ^L , C-myc ^L , Adfp ^L , Cyb5M ^L , Gsk3b ^L , Cry2 ^L , P53 ^L , Rac1 ^L , Nfkb1 ^L , Cyp51a1 ^{HY} , Rnh1 ^{HY} , Adfp ^{HY} , Abat ^{HY} , Bmal1 ^{HY} , Bcl2 ^S
(0, 0, -1) (16 cases)	Rps16 ^B , Bmal1 ^B , Bhlhb2 ^B , Bid ^B , Tgfb1i4 ^B , Cyp51a1 ^L , Rhoc ^L , Hif1a ^L , Acaa2 ^{HY} , Clock ^{HE} , c-fos ^{HE} , Clock ^{HY} , Lgmn ^S , Mapk14 ^S , Hif1a ^S , Foxo1a ^S
(1, 0, 0) (15 cases)	Cry1 ^B , Bcl2l1-xL ^B , Nfkb1 ^B , Gsk3a ^L , Map2k1 ^L , Map3k5 ^L , c-fos ^L , Tgfb1 ^{HE} , Scd ^{HY} , Map3k1 ^{HY} , P53 ^{HY} , Nfkb1 ^{HY} , Bid ^S , Birc2 ^S , Tgfb2 ^S
(1, 0, -1) (13 cases)	P53 ^B , Clock ^L , Mapk14 ^L , Map3k1 ^L , c-jun ^L , Map3k1 ^{HE} , Birc2 ^{HE} , Tgfb1i4 ^{HE} , Mapk14 ^{HY} , Hsp90ab1 ^S , Map3k1 ^S , c-jun ^S , c-fos ^S
(-1, 0, 0) (10 cases)	Hsl ^B , Otc ^L , Dhhrs4 ^L , Ryr2 ^{HE} , Atp2a2 ^{HE} , Fabp4 ^{HE} , Cs ^{HE} , Bhlhb2 ^{HE} , Acacab ^{HY} , c-jun ^{HY}
(-1, 0, 1) (6 cases)	Cpt1b ^B , Acaa1 ^L , Cox5b ^L , Pdk2 ^{HE} , Hist1h2al ^{HE} , Gnao1 ^{HY}
(-1, -1, -1) (4 cases)	Mgst1 ^L , Mapk14 ^{HE} , Glud1 ^{HY} , Tgfb2 ^{HY}
(-1, 1, 1) (3 cases)	Pck1 ^B , Apc ^L , Hist1h2al ^{HY}
(1, -1, -1) (3 cases)	c-fos ^B , Gsy2 ^L , Tgfb1i4 ^L
(1, 1, 1) (1 case)	Mdh2 ^{HY}

Differential gene expression patterns in 3-stage analysis are represented by (X_{A-T}, X_{A-PR}, X_{T-PR}), where X_{I-J} = 1 if the gene expression in stage I is significantly higher than that in stage J; -1 if significantly lower; 0 if not significantly different; I, J = A (arousal), T (torpor), PR (postreproduction). $P < 0.05$ in post hoc Tukey's test is used as the criterion for significance. The superscripts on the gene symbols: B, L, HE, S, HY represent brown adipose tissue (BAT), liver, heart, skeletal muscle, and hypothalamus, respectively.

a “seasonal” pattern of differential expression with a significant increase or decrease in expression during both arousal and torpor compared with PR but no significant difference between arousal and torpor. Patterns (-1, 0, 1) with 6 cases and (1, 0, -1) with 13 cases correspond to an “arousal-recovered” pattern of expression with significant increases or decreases during torpor compared with PR followed by a return to a level of expression similar to PR during arousal. Pattern (1, 1, 0) with 17 cases corresponds to an “arousal-specific” pattern of expression with over-expression seen only in arousal compared with both torpor and PR.

In real-time PCR assay, we had enough samples from animals in the torpor-arousal cycle to further investigate the modulation of gene expression in each stage. Four-stage analysis on the real-time PCR results among EA, LA, ET, and LT in all five tissues was carried out by one-way ANOVA followed by post hoc Tukey's test. PR is not included in this step of analysis to avoid those genes already identified as differentially expressed in the seasonal pattern by the three-stage analysis. The complete results of four-stage analysis in all tissues are given in Table S5. We use $X > Y$ or $X < Y$ to denote that the gene expression in state X is significantly ($P < 0.05$) higher or lower than in state Y in post hoc Tukey's test, where X, Y = (A, T, PR) in three-stage analysis and (EA, LA, ET, LT) in four-stage analysis. Among all step-wise comparisons between the four stages sampled during the torpor-arousal cycle in all five tissues, the most significant differences were seen in the transition from LA to EA (50 cases), followed

by the transition from early to late arousal (40 cases) and the transition from LA to ET (37 cases). The transition from early to late torpor showed the fewest differences with only 9 cases, including increased expression of *Glud1* (liver), *CGI-69* (liver), *Fmo5* (BAT), *Prdx6* (heart) from early to late torpor and decreased expression of *Bckdha* (BAT), *Cry1* (BAT), *Pdk2* (heart), *Rnh1* (heart), and *Mapk14* (skeletal muscle) from early to late torpor.

We classify genes tested in real-time PCR according to their biological functions and display real-time PCR results in liver in the form of a heat map (Fig. 3) corresponding to stages of animals and functional categories of tested genes. The heat maps of other tissues are included in the supplemental materials. We used Fisher's exact test to investigate the over- or underrepresentation of each functional category in each group of pair-wise comparisons in three- and four-stage analysis. The results are shown in Tables 3 and 4. We summarize the results of differential gene expression for important functional categories below.

Metabolism. Our results suggest that the most prominent seasonal change during hibernation is a shift of metabolic fuel use from carbohydrate catabolism to fatty acid catabolism. Comparing torpor to PR, this is manifested by the significant underexpression of glycolytic enzymes including *Hk4* in liver and *Pfkms* and *Pkm2* in skeletal muscle, overexpression of *Pdk4* in BAT, heart, and skeletal muscle, and overexpression of fatty acid catabolic genes: *Cpt1a*, *Cpt1b*, *Acadm*, *Acadvl*, *Hadha*, and *Cact* in BAT, *Fabp1*, *Acaa1*, *Acadvl*, *Hadhsc*, and *Cpt1a*

Table 3. Distribution of differentially expressed genes among tissues and pathways in three-stage analysis in real-time PCR assay

Tissues and Pathways	Tested	ANOVA $P < 0.05$	A > T	A < T	A > PR	A < PR	T > PR	T < PR
Liver	129	79	20	6	42	19	26	24
BAT	96	37	6	3	15	7	16	10
Heart	99	45	4	8	13	13	20	14
Hypothalamus	95	54	11	6	21	18	18	16
Skeletal muscle	76	33	8	0	11	8	10	13
All	495	248	49	23	102	65	90	77
Fatty acid catabolism	43	25	0* \downarrow	4	11	2	20 \ddagger \uparrow	3
Circadian rhythm	40	17	5	1	7	0 \ddagger \downarrow	4	5
MAPK pathway	40	22	8* \uparrow	1	7	4	4	9
Cell growth and apoptosis	115	55	22 \ddagger \uparrow	2	11 \ddagger \downarrow	22* \uparrow	2 \ddagger \downarrow	28 \ddagger \uparrow

P value < 0.05 in 1-way ANOVA was used as the criterion for differential expression. A, arousal; T, torpor; PR, postreproduction; EA, early arousal; LA, late arousal; ET, early torpor; LT, late torpor. $X > Y$ or $X < Y$ denotes that the gene expression in X is significantly ($P < 0.05$) higher or lower than in Y in post hoc Tukey's test, where X, Y = (A, T, PR). Fisher's exact test was used to estimate the over- (\uparrow) or underrepresentation (\downarrow) of each pathway in $X > Y$ or $X < Y$ groups. * $0.01 < P < 0.05$, $\ddagger 0.001 < P < 0.01$, and $\ddagger P < 0.001$.

in liver, *Cpt1a*, *Cpt1b*, *Cact*, and *Fabp3* in heart, *Acs13*, and *Acadm* in hypothalamus, *Cpt1a*, *Cpt1b*, and of *Hadhs* in skeletal muscle. Fatty acid catabolic genes are significantly overrepresented in the T > PR group (20 cases, $P < 0.001$, Fisher's exact test). In contrast, genes involved in fatty acid biosynthesis: *Scd*, *Acacb*, *Elovl6*, *Sc4mol*, and *Agpat3* in liver and *Scd* in BAT are significantly underexpressed in torpor compared with PR. TCA cycle genes including *Idh2* in liver and BAT and *Mdh2* in liver, BAT, and hypothalamus are significantly overexpressed in torpor compared with PR. Genes involved in gluconeogenesis: *Pck1* in BAT and *Pck1*, *Pck2*, and *G6pd* in liver are also significantly overexpressed. In liver, *Ugp2* and *Gys2* (glycogen synthesis) are significantly underexpressed whereas *Pygb* (glycogen breakdown) is overexpressed in torpor compared with PR. Among the genes involved in amino acid metabolism, *Arg1* (urea cycle) in liver, *Bckdhb* (branched chain amino acid catabolism) in heart, *Hpd* (phenylalanine catabolism) in heart, *Glud1* (glutamate metabolism) in hypothalamus are significantly underexpressed, whereas *Glud1* in liver, *Got2* (aspartate aminotransferase) in liver and heart, and *Bckdhb* in hypothalamus are significantly overexpressed in torpor compared with PR.

During the torpor-arousal cycle, most metabolic genes do not show significant changes of expression. However, there is a significant decrease in mRNA levels for a subset of metabolic genes during the transition from torpor to arousal. Fatty acid

catabolic genes are significantly underrepresented in the A > T group (0 case, $P = 0.01$) and overrepresented in the EA < LT group (6 cases, $P = 0.01$). Other metabolic genes including *Otc*, *Cox5b*, and *Dhrs4* in liver, *Pck1* in BAT, *Cs* in heart, and *Glud1* and *Acacb* in hypothalamus show similar underexpression in arousal compared with torpor. However, *Gys2* (glycogen biosynthesis) is overexpressed in arousal compared with torpor.

Circadian rhythm genes. Comparing torpor to PR, circadian rhythm genes show a variety of patterns, including significantly increased expression of *Per1* (liver and hypothalamus), *Cry2* (hypothalamus), and *Bhlhb2* (hypothalamus) and decreased expression of *Clock* (liver, heart, and hypothalamus), *Bmal1* (BAT), and *Bhlhb2* (BAT) in torpor compared with PR. During the torpor-arousal cycle, there is a generally consistent pattern that *Cry1* (BAT), *Cry2* (BAT and liver), *Clock* (liver), and *Bmal1* (hypothalamus) are significantly overexpressed whereas only *Bhlhb2* (heart) is underexpressed in arousal compared with torpor. *Per1* has significantly higher expression in EA than LA in all five tissues. *Cry1* (liver, BAT, and hypothalamus), *Cry2* (liver and BAT), *Bmal1* (heart), and *Per1* (skeletal muscle) are significantly overexpressed in EA compared with both LA and LT. In fact, circadian genes are overrepresented in the EA > LA group (12 cases, $P < 0.001$) and the EA > LT group (8 cases, $P = 0.001$), indicating a peak of circadian gene expression during early arousal.

Table 4. Distribution of differentially expressed genes among tissues and pathways in four-stage analysis in real-time PCR assay

Tissues and Pathways	Tested	ANOVA $P < 0.05$	EA > LA	EA < LA	EA > LT	EA < LT	LA > ET	LA < ET	ET > LT	ET < LT
Liver	129	43	12	1	17	2	7	4	2	0
BAT	96	17	3	1	4	7	3	0	1	2
Heart	99	26	10	0	3	3	1	3	1	2
Hypothalamus	95	20	2	2	2	8	6	2	0	0
Skeletal muscle	76	22	1	8	3	1	11	0	0	1
All	495	128	28	12	29	21	28	9	4	5
Fatty acid catabolism	43	11	0	1	0	6 \ddagger \uparrow	0	0	0	0
Circadian rhythm	40	18	12 \ddagger \uparrow	1	8 \ddagger \uparrow	0	3	3* \uparrow	0	1
MAPK pathway	40	11	2	2	3	1	6* \uparrow	0	0	1
Cell growth apoptosis	115	39	10	2	13* \uparrow	1* \downarrow	13* \uparrow	1	0	0

P value < 0.05 in 1-way ANOVA was used as the criterion for differential expression. $X > Y$ or $X < Y$ denotes that the gene expression in X is significantly ($P < 0.05$) higher or lower than in Y in post hoc Tukey's test, where X, Y = (EA, LA, ET, LT). Fisher's exact test was used to estimate the over- (\uparrow) or underrepresentation (\downarrow) of each pathway in $X > Y$ or $X < Y$ groups. * $0.01 < P < 0.05$, $\ddagger 0.001 < P < 0.01$, and $\ddagger P < 0.001$.

MAP kinase genes. *Map3k1* in liver, heart, and skeletal muscle, *Mapk14* in liver, heart, skeletal muscle, and hypothalamus, *Map2k1* and *Map3k5* in hypothalamus are significantly underexpressed and *Mapk3* in heart and skeletal muscle, *Raf1* in liver, and *Map3k5* in heart are significantly overexpressed in torpor compared with PR. During the torpor-arousal cycle, *Map3k1* in liver, heart, skeletal muscle, and hypothalamus, *Mapk14* in liver and hypothalamus, *Map2k1* and *Map3k5* in liver are significantly overexpressed, whereas only *Mapk14* in heart is underexpressed in arousal compared with torpor. *Raf1* in liver and heart is significantly overexpressed whereas *Raf1* and *Map3k1* in skeletal muscle are underexpressed in EA compared with LA. *Map3k1* in liver, skeletal muscle, and hypothalamus, *Mapk14* in liver and skeletal muscle, and *Raf1* in skeletal muscle are significantly overexpressed in LA compared with ET. MAP kinase genes are overrepresented in the A > T group (8 cases, $P = 0.05$) and the LA > ET group (6 cases, $P = 0.03$).

Cell growth and apoptosis genes. We tested 23 genes involved in cell growth and apoptosis in all five tissues using real-time PCR, including oncogenes like *c-myc*, *c-fos*, and *c-jun* and tumor suppressor genes like *p53*. Genes involved in cell growth and apoptosis are significantly overrepresented in the T < PR group (28 cases, $P = 0.005$) and underrepresented in the T > PR group (2 cases, $P < 0.001$). They are also significantly overrepresented in the A > T group (22 cases, $P < 0.001$). This indicates that the mRNA levels of genes involved in cell growth and apoptosis decrease during torpor compared with PR and recover during arousal compared with torpor. This recovery is also manifested in the significant overrepresentation of these genes in the EA > LT group (13 cases, $P = 0.01$) and the LA > ET group (13 cases, $P = 0.01$).

Molecular transport. Genes for molecular transporters are significantly overexpressed in either arousal or torpor compared with PR. These include: *Alb* (steroid, fatty acid, and thyroid hormone transport) in liver; *Slc16a12* or *Mct12* (lactate, pyruvate, and ketone body transport) in liver; *Laptm4a* (small molecule transport) in liver and hypothalamus; *Trappc5* (vesicle-mediated transport) in liver; *Abcb7* (heme transport) in liver; *Coll8a1* (phosphate transport) in liver; *Tf* (ferric ion transport) in liver and hypothalamus. These changes of gene expression could indicate that transport capacities are increased to distribute various molecular "cargos" more efficiently in response to the limited supplies available during hibernation. There are no significant changes of expression in molecular transporters during the torpor-arousal cycle.

Xenobiotic metabolism. Genes involved in xenobiotic metabolism or detoxification are significantly underexpressed in either torpor or arousal compared with PR. These include: *Cyp1a2* and *Cyp51a1* (members of cytochrome P450 enzymes) in liver; *Fmo5* (drug, cholesterol, and steroid metabolism) in liver and BAT; *Ces1* (drug metabolism) in liver. Most of these do not show significant changes in gene expression during the torpor-arousal cycle. Only *Cyp51a1* in hypothalamus is overexpressed in arousal compared with torpor.

Antioxidant genes. Antioxidant genes *Cat*, *Prdx6*, and *Mgst1* in liver and *Prdx6* and *Sepp1* in BAT are significantly underexpressed in both arousal and torpor compared with PR. Most antioxidant genes do not show significant changes in gene expression during the torpor-arousal cycle except that *Mgst1* in

liver is significantly underexpressed in arousal compared with torpor.

DISCUSSION

Metabolic fuel shift. In our study, significant seasonal changes of metabolic gene expression in multiple tissues, including underexpression of glycolytic genes and overexpression of fatty acid catabolic genes, are consistent with the paradigm that energy catabolism shifts from carbohydrate substrates to fatty acids during hibernation. *Pdk4* inactivates pyruvate dehydrogenase by phosphorylation and, therefore, blocks the conversion of pyruvate to acetyl-CoA in carbohydrate catabolism. *Pdk4* has previously been shown to be overexpressed during torpor in heart, skeletal muscle, and white adipose tissue of thirteen-line ground squirrels (2, 13). In our study of arctic ground squirrels, *Pdk4* is overexpressed during torpor in heart, skeletal muscle, and BAT. *Pck1*, a key enzyme involved in gluconeogenesis, is overexpressed in liver in both torpor and arousal compared with PR and in BAT in torpor compared with PR, suggesting an increase in gluconeogenesis during hibernation. The substrate of gluconeogenesis in BAT is most likely glycerol as hormone-sensitive lipase (*Hsl*) cleaves triglyceride into free fatty acid and glycerol. Fatty acids fuel NST in BAT. Glycerol is phosphorylated by glycerol kinase into glycerol 3-phosphate, which is subsequently oxidized by glycerol-3-phosphate dehydrogenase into dihydroxyacetone phosphate, which enters gluconeogenesis. This is consistent with our finding that glycerol-3-phosphate dehydrogenase 1 (*Gpd1*) has an expression profile similar to *Hsl* in BAT. In liver, another source of gluconeogenesis can come from amino acid metabolism. In amino acid metabolism, aminotransferase and glutamate dehydrogenase together convert amino acid into α -ketoglutarate, which can enter the TCA cycle and gluconeogenesis. We have shown overexpression of aminotransferase and glutamate dehydrogenase together with underexpression of urea cycle genes in liver during torpor in our study. This may lead to a redirection of amino acids from urea cycle to gluconeogenesis and the TCA cycle. Overexpression of gluconeogenesis enzymes together with aminotransferases and glutamate dehydrogenase has also been observed in mouse liver under caloric restriction (28). Gluconeogenesis in liver can provide glucose in a fasting animal to organs like brain and red blood cells, where glucose is the major energy source. Increased availability of glucose in BAT may also be necessary to support increased rates of NST for arousal and during steady-state torpor in arctic ground squirrels when they are defending a gradient between body and ambient temperatures (12).

Adipocyte differentiation-related protein or adipophilin (*Adfp*) is associated with fatty acid accumulation in lipid droplet in cells and is expressed in a variety of tissues (17, 18). *Adfp* is overexpressed in both torpor and arousal compared with PR in BAT, heart, and skeletal muscle and overexpressed in arousal compared with both torpor and PR in liver and hypothalamus. In our previous study (59), *Adfp* was found to be overexpressed in BAT of animals in torpor compared with summer-active animals, suggesting that it serves to enhance the thermogenic capacity in BAT. Overexpression of *Adfp* in multiple tissues may indicate an important role in enhancing fatty acid metabolism during hibernation, even in the brain.

During the torpor-arousal cycle, a decrease of mRNA levels for a subset of metabolic genes such as *Pck1* in BAT is most significant when arctic ground squirrels enter EA from LT. As transcript levels for these metabolic genes are maintained at a high level during torpor compared with PR, a decrease in their mRNA levels during EA may result from the high metabolic rate and increased thermogenesis during warming that leads to rapid mRNA translation and turnover. The mRNA levels of most of these metabolic genes show a trend toward recovery later in the arousal stage although it is generally not statistically significant, $P = 0.18$ in EA vs. LA comparison for *Pck1* in BAT for example. This suggests that mRNA lost in EA may be replenished gradually later in the arousal episode or during reentry into torpor.

Uncoupling proteins. Probes for all three homologs of uncoupling proteins, *Ucp1*, *Ucp2*, and *Ucp3*, were included on our bead arrays. *Ucp1* is detected only in BAT and is not significantly differentially expressed in our analysis. *Ucp2* is detected in BAT and heart and significantly overexpressed in heart in both torpor and arousal compared with PR, whereas *Ucp3* is not detected in any tissue in this experiment. The functions of *Ucp2* and *Ucp3* remain unclear, although current evidence indicates they are unlikely to be involved in NST (14). In other species, *Ucp2* is expressed in multiple tissues including white adipose tissue (WAT), spleen, and heart, whereas *Ucp3* is expressed mainly in skeletal muscle. Boss et al. (7) showed that *Ucp2* is overexpressed in BAT, heart, and soleus muscle of rat during cold exposure. *Ucp2* is overexpressed in WAT and *Ucp3* in skeletal muscle in hibernating arctic ground squirrels (8). The overexpression of *Ucp2* has been suggested to be part of an antioxidant defense response in the heart under oxidative stress (52) and/or ischemia (39). In our experiment, the *CGI-69* protein gene is significantly overexpressed in both torpor and arousal compared with PR in BAT and heart. Yu et al. (61) showed that *CGI-69* is a mitochondrial carrier and overexpressed twofold in the BAT of mice during cold exposure. They proposed that *CGI-69* is a homolog of uncoupling proteins, although transfection of *CGI-69* failed to change mitochondrial membrane potential casting doubt on its uncoupling activity.

RNA and protein protection. RNA binding motif protein 3 (*Rbm3*) is overexpressed during torpor in liver, heart, and brain of golden-mantled ground squirrels (58). Here we show that *Rbm3* is overexpressed in both torpor and arousal compared with PR in all tissues that we studied. As RNA binding proteins may have general functions such as RNA protection or translation inhibition, their overexpression is consistent with the observation that mRNA transcripts are protected from degradation during torpor (32). In further support of this, RNase inhibitor H (*Rnh1*) with RNA protection function is significantly overexpressed in both arousal and torpor compared with PR in heart and skeletal muscle and overexpressed in arousal compared with both torpor and PR in hypothalamus.

Two heat shock proteins, *Hspe1* and *Hsp90ab1*, were underexpressed in BAT of torpid compared with summer-active arctic ground squirrels in our previous study (59). In this study, *Hsp90ab1* is significantly underexpressed in heart and skeletal muscle in torpor compared with PR. However, *Hspe1* is significantly underexpressed in liver but overexpressed in heart in torpor compared with PR. In addition, *Hsp90ab1* is significantly overexpressed in liver and skeletal muscle in arousal

compared with torpor, whereas no significant difference between arousal and torpor is found in *Hspe1* expression in any tissue. The overexpression of *Hsp90ab1* during arousal may help to maintain proper configuration of the proteins as body temperature increases during early stage of arousal. It is unclear why *Hsp90ab1* and *Hspe1* are underexpressed in certain tissues when body temperature is near 0°C during torpor. The different expression patterns between *Hsp90ab1* and *Hspe1* during hibernation may indicate subtle functional differences between these two heat shock proteins.

Tissue-specific protection mechanism. The arctic ground squirrel heart maintains regular contractile functions during torpor as heart rate slows to ~2% of euthermic rate and tissue temperatures decrease to near 0°C, whereas in nonhibernating mammals cardiac arrhythmia and ventricular fibrillation occur under only shallow hypothermia. In heart, we found that the gene for myosin light polypeptide 6 (*Myl6*) is significantly overexpressed in both torpor and arousal compared with PR. Change of myosin isoform composition may enhance the contractility of the hibernating heart (41–43). Brauch et al. (10) found underexpression of myosin light polypeptide 3, ventricular isoform (*Myl3*) and overexpression of myosin heavy polypeptide 6 (*Myh6*) in the heart of thirteen-line ground squirrels in torpor compared with summer-active animals, whereas Fahlman et al. (22) found that *Myl3* was overexpressed in hibernating golden-mantled ground squirrels. Maintenance of intracellular Ca^{2+} homeostasis is also important for contractile function of heart at low temperatures (35, 56). *Atp2a2*, a Ca^{2+} pump located on the sarcoplasmic/endoplasmic reticulum (SR/ER) membrane and responsible for Ca^{2+} removal from cytosol, has been shown to be overexpressed during torpor in several hibernating species (10, 60). In our study, *Atp2a2* is significantly underexpressed in arousal compared with torpor. In addition, ryanodine receptor 2 (*Ryr2*), a Ca^{2+} release channel on SR membrane, is also significantly underexpressed in arousal compared with torpor. This could be due to Ca^{2+} load returning to normal level at euthermic body temperature in the heart during arousal. *Tmed4* is significantly overexpressed in both arousal and torpor compared with PR. *Tmed4* has been shown to be a member of a transmembrane protein complex on ER with Ca^{2+} binding capability (55). This may further contribute to the enhanced Ca^{2+} clearance from cytosol to avoid Ca^{2+} overload in cold hearts during torpor.

In hypothalamus, *Abat* is significantly overexpressed in arousal compared with both torpor and PR. *Abat* is responsible for catabolism of gamma-aminobutyric acid (GABA), an important inhibitory neurotransmitter. The overexpression of *Abat* may lead to decreased GABA levels in hypothalamus during arousal. Lust et al. (37) observed elevated GABA levels in the brains of hibernating hamsters and suggested they acted as a neuronal depression mechanism, whereas Osborne et al. (45), using quantitative microdialysis, showed that GABA is decreased in the striatum of arctic ground squirrel in torpor. Overexpression of *Abat* in the hypothalamus during arousal could be important for control of NST in BAT during arousal, since the inhibitory signal from preoptic/anterior hypothalamus to ventromedial nucleus is mediated by GABA along the thermoregulatory pathway from hypothalamus to BAT (14).

In skeletal muscle, carbonic anhydrase III (*Ca3*) and creatine kinase muscle (*Ckm*) are significantly underexpressed in both arousal and torpor compared with PR. Interestingly, Jagoe

et al. (31) showed that mRNA levels of *Ca3* and *Ckm* were significantly reduced in the skeletal muscle of fasting mice experiencing muscle atrophy. Furthermore, serum levels of both *Ca3* and *Ckm* proteins are significantly increased in human patients with muscle dystrophy, especially Duchenne muscle dystrophy, which is most likely due to the loss of these proteins in skeletal muscle (40). *Ca3* has an antioxidant function (62); therefore, its underexpression during hibernation is consistent with the underexpression of other antioxidant genes. Our results indicate that skeletal muscles in hibernating arctic ground squirrels undergo gene expression changes that are similar to those in atrophying muscles.

Circadian rhythm. In mammals, circadian rhythms are controlled by negative feedback loops formed by a set of key circadian genes: *Per* family (*Per1/Per2/Per3*), *Bmal1*, *Cry* family (*Cry1/Cry2*), *Clock*, *Timeless*, *Dec1/Dec2*, and *Rev-erba*. (48). At the core of the negative feedback loop, *Bmal1* and *Clock* proteins form a complex that positively regulates the transcription of *Per* and *Cry* genes, whereas *Per* and *Cry* proteins inhibit *Bmal1/Clock* activity. In mouse, the mRNA levels of *Per* and *Cry* reach the peak at 12–15 h (dusk) and the trough at 18–21 h (dawn) in 12L:12D cycles. In contrast, the mRNA levels of *Bmal1* and *Clock* reach the peak at 0 h (dawn) and the trough at 12–15 h (dusk), showing antiphase to *Per* and *Cry* gene expression. The persistence or absence of circadian rhythms during hibernation remains controversial (30). Grahn et al. (26) observed that circadian body temperature rhythms persist during torpor in golden-mantled ground squirrels although at a greatly dampened amplitude compared with euthermia. In a recent study, Revel et al. (49) showed that the mRNA levels of key circadian genes such as *Per1*, *Per2*, and *Bmal1* no longer display a 24 h rhythm during torpor in the suprachiasmatic nucleus of European hamster (*Cricetus cricetus*), suggesting a suppressed circadian rhythm during torpor.

In arctic ground squirrels, we observe a significant rise in the mRNA levels of key circadian rhythm genes in all five tissues as animals arouse from torpor, suggesting the resumption of circadian rhythm during arousal. This is consistent with the observation of Revel et al (49). In our study, *Per1* in heart and hypothalamus and *Per3* in heart is significantly underexpressed in LA compared with ET, whereas *Clock* in liver and skeletal muscle are significantly overexpressed. *Per1* in liver and hypothalamus and *Cry2* in hypothalamus are significantly overexpressed in torpor compared with PR, whereas *Bmal1* in BAT and *Clock* in heart, liver, and hypothalamus are significantly underexpressed. These results are consistent with the antagonizing nature between *Per/Cry* and *Bmal1/Clock*. *Timeless* is the only “circadian” gene showing no significant modulation in any tissues studied during hibernation, consistent with the suggestion that *Timeless* plays no role in circadian rhythm in mammals but is rather a developmental gene (25).

Cell growth and apoptosis. Genes involved in cell growth and apoptosis are significantly underexpressed in torpor compared with PR. They also showed significant overexpression in the early or late arousal during the torpor-arousal cycle, similar to circadian rhythm genes. Immediate early genes *c-myc*, *c-jun*, and *c-fos* are key transcription factors regulating cell cycle progression, apoptosis, and cellular transformation. Their significant overexpression during EA is consistent with a previous observation that *c-fos* and *c-jun* were overexpressed during arousal in brain and other tissues in golden-mantled ground

squirrel (6, 44). The expression of tumor suppressor gene *p53* reaches its peak in LA in liver, skeletal muscle, and hypothalamus. The time delay between oscillation patterns of oncogenes like *c-myc*, *c-jun*, and *c-fos* and that of tumor suppressor gene *p53* may be important for the cells to exit cell cycles and/or for cells with DNA damage to undergo apoptosis before animals reenter torpor. There is experimental evidence that the cell cycle is blocked at G₂ or late S phase during torpor but resumes during arousal in intestinal epithelial cells (16, 33). It was proposed that this prevents cells from possible damage in mitosis under hypothermia accompanying hibernation (33). Fleck and Carey (23) observed the decrease of proapoptotic proteins like p53 and increase of antiapoptotic proteins like Bcl-xL in intestinal mucosa of hibernating thirteen-line ground squirrels compared with summer animals. Our results showed a variety of patterns for both pro- and antiapoptotic genes comparing torpor and arousal with PR depending on the tissue type. During the torpor-arousal cycle, we found a generally common pattern for mRNA levels of both pro- and antiapoptotic genes being higher in arousal than torpor.

Differences between mRNA and protein levels. Galster and Morrison (24) showed that blood glucose and liver glycogen are replenished during arousal through gluconeogenesis in arctic ground squirrels, and they estimated that three-fourths of new glucose was synthesized from fat and one-fourth from protein. Whitten and Klain (57) showed that protein catabolism increases during arousal in thirteen-line ground squirrels. Our results, however, show no significant variation of mRNA levels of genes involved in either gluconeogenesis or amino acid metabolism in liver during the torpor-arousal cycles in environmental temperatures >0°C. There is even significant underexpression of genes involved in gluconeogenesis in BAT in arousal compared with torpor. Antioxidants are thought to form an important defense from damage following reperfusion during arousal from torpor (20). However, here too we observed no significant changes of gene expression of antioxidant genes in arousal compared with torpor. These contradictions may reflect the fact that changes in mRNA levels do not necessarily correlate with changes in protein levels and/or protein activities, particularly during torpor-arousal cycles. The mRNA transcripts for genes involved in gluconeogenesis or amino acid metabolism may have been stored during torpor and readily made into proteins when needed during arousal. Antioxidant genes may remain at similar levels of mRNA transcripts during arousal but can be activated through translational regulation and/or posttranslational modification. These considerations may explain the disparities between our mRNA expression data and some previous biochemical and physiological studies and emphasize the need for complete studies of gene expression and protein synthesis and activation for understanding the regulation of hibernation.

Conclusion

Our study is the most systematic gene expression study on hibernation thus far including detailed hibernation stages and a wide range of tissues in a spontaneously arousing hibernator. Our results support that a shift from carbohydrate to fatty acid catabolism is the major theme of gene expression reprogramming during hibernation in multiple tissues. The comparisons among arousal, torpor, and PR reveal that global gene expres-

sion in arousal is closer to that in torpor than that in PR, i.e., the seasonal difference in gene expression is more significant than the variation seen during the torpor-arousal cycle. However, the variation of gene expression during multiple stages of torpor-arousal cycle exhibits a complex pattern. We observed a significant drop in expression of a subset of metabolic genes during the transition from LT to EA. We propose that this is due to rapid turnover of mRNA transcripts during the energetically costly EA phase. We also observed a sharp rise of expression at early or late arousal stages for genes related to circadian rhythm and cell growth and apoptosis. Based on these observations, we propose that circadian rhythm and cell cycle resume during arousal. Certain disparities between our data and previous biochemical and physiological studies, especially during the torpor-arousal cycle, point to the importance of studying molecular changes at all levels to fully understand the molecular mechanisms of hibernation.

ACKNOWLEDGMENTS

We thank Dr. Michael Schlador of Illumina for technical support and Dr. Kelly Drew of the Institute of Arctic Biology for providing some of the arctic ground squirrels used in this experiment and for helpful comments on the manuscript. We are grateful for the helpful comments from anonymous referees.

GRANTS

We acknowledge the support from National Institutes of Health Grant RR-16466-01 (T. G. Marr), National Science Foundation (NSF) Grant EPS-0092040 (T. G. Marr), University of Alaska Foundation (T. G. Marr and B. M. Barnes), National Basic Research Program of China Grant 2006CB910700, and NSF Grant OPP 0117104 and US Army Medical Research and Materiel Command Grant #05178001 (B. M. Barnes).

REFERENCES

- Altschul SF, Gish W, Miller W, Myers EW, Lipman DJ. Basic local alignment search tool. *J Mol Biol* 215: 403–410, 1990.
- Andrews MT, Squire TL, Bowen CM, Rollins MB. Low-temperature carbon utilization is regulated by novel gene activity in the heart of a hibernating mammal. *Proc Natl Acad Sci USA* 95: 8392–8397, 1998.
- Barnes BM. Freeze avoidance in a mammal: body temperatures below 0 degree C in an Arctic hibernator. *Science* 244: 1593–1595, 1989.
- Barnes BM, Kretzmann M, Licht P, Zucker I. Influence of hibernation on testis growth and spermatogenesis in the golden-mantled ground squirrel, *Spermophilus lateralis*. *Biol Reprod* 35: 1289–1297, 1986.
- Barnes BM, Omtzigt C, Daan S. Hibernators periodically arouse in order to sleep. In: *Life in the Cold III: Ecological, Physiological, and Molecular Mechanisms*. edited by Carey C, Florant GL, Wunder BA, Horwitz B. Boulder, CO: Westview, 1993, p. 555–558.
- Bitting L, Sutin EL, Watson FL, Leard LE, O'Hara BF, Heller HC, Kilduff TS. C-fos mRNA increases in the ground squirrel suprachiasmatic nucleus during arousal from hibernation. *Neurosci Lett* 165: 117–121, 1994.
- Boss O, Samec S, Dulloo A, Seydoux J, Muzzin P, Giacobino JP. Tissue-dependent upregulation of rat uncoupling protein-2 expression in response to fasting or cold. *FEBS Lett* 412: 111–114, 1997.
- Boyer BB, Barnes BM, Lowell BB, Grujic D. Differential regulation of uncoupling protein gene homologues in multiple tissues of hibernating ground squirrels. *Am J Physiol Regul Integr Comp Physiol* 275: R1232–R1238, 1998.
- Boyer BB, Barnes BM. Molecular and metabolic aspects of mammalian hibernation. *Bioscience* 49: 713–724, 1999.
- Brauch KM, Dhruv ND, Hanse EA, Andrews MT. Digital transcriptome analysis indicates adaptive mechanisms in the heart of a hibernating mammal. *Physiol Genomics* 23: 227–234, 2005.
- Buck CL, Barnes BM. The annual cycle of body condition and hibernation in free-living arctic ground squirrels. *J Mammal* 80: 430–442, 1999.
- Buck CL, Barnes BM. Effects of ambient temperature on metabolic rate, respiratory quotient, and torpor in an arctic hibernator. *Am J Physiol Regul Integr Comp Physiol* 279: R255–R262, 2000.
- Buck MJ, Squire TL, Andrews MT. Coordinate expression of the PDK4 gene: a means of regulating fuel selection in a hibernating mammal. *Physiol Genomics* 8: 5–13, 2002.
- Cannon B, Nedergaard J. Brown adipose tissue: function and physiological significance. *Physiol Rev* 84: 277–359, 2004.
- Carey HV, Andrews MT, Martin SL. Mammalian hibernation: cellular and molecular responses to depressed metabolism and low temperature. *Physiol Rev* 83: 1153–81, 2003.
- Carey HV, Martin SL. Preservation of intestinal gene expression during hibernation. *Am J Physiol Gastrointest Liver Physiol* 271: G805–G813, 1996.
- Chang BH, Li L, Paul A, Taniguchi S, Nannegari V, Heird WC, Chan L. Protection against fatty liver but normal adipogenesis in mice lacking adipose differentiation-related protein. *Mol Cell Biol* 26: 1063–1076, 2006.
- Chang BHJ, Chan L. Regulation of Triglyceride Metabolism. III. Emerging role of lipid droplet protein ADFP in health and disease. *Am J Physiol Gastrointest Liver Physiol* 292: G1465–G1468, 2007.
- Daan S, Barnes BM, Strijkstra AM. Warming up for sleep? Ground squirrels sleep during arousals from hibernation. *Neurosci Lett* 128: 265–268, 1991.
- Drew KL, Rice ME, Kuhn TB, Smith MA. Neuroprotective adaptations in hibernation: therapeutic implications for ischemia-reperfusion, traumatic brain injury and neuroprotective diseases. *Free Radic Biol Med* 31: 563–573, 2001.
- Eisen MB, Spellman PT, Brown PO, Botstein D. Cluster analysis and display of genome-wide expression patterns. *Proc Natl Acad Sci USA* 95: 14863–14868, 1998.
- Fahlman A, Storey JM, Storey KB. Gene up-regulation in heart during mammalian hibernation. *Cryobiology* 40: 332–342, 2000.
- Fleck CC, Carey HV. Modulation of apoptotic pathways in intestinal mucosa during hibernation. *Am J Physiol Regul Integr Comp Physiol* 289: R586–R595, 2005.
- Galster W, Morrison PR. Gluconeogenesis in arctic ground squirrels between periods of hibernation. *Am J Physiol* 228: 325–330, 1975.
- Gotter AL, Manganaro T, Weaver DR, Kolakowski LF Jr, Possidente B, Sriram S, MacLaughlin DT, Reppert SM. A time-less function for mouse timeless. *Nat Neurosci* 3: 755–756, 2000.
- Grahn DA, Miller JD, Houng VS, Heller HC. Persistence of circadian rhythmicity in hibernating ground squirrels. *Am J Physiol Regul Integr Comp Physiol* 266: R1251–R1258, 1994.
- Gunderson KL, Kruglyak S, Graige MS, Garcia F, Kermani BG, Zhao C, Che D, Dickinson T, Wickham E, Bierle J, Doucet D, Milewski M, Yang R, Siegmund C, Haas J, Zhou L, Oliphant A, Fan JB, Barnard S, Chee MS. Decoding Randomly Ordered DNA Arrays. *Genome Res* 14: 870–877, 2004.
- Hagopian K, Ramsey JJ, Weindruch R. Caloric restriction increases gluconeogenic and transaminase enzyme activities in mouse liver. *Exp Gerontol* 38: 267–278, 2003.
- Heldmaier G, Ortman S, Elvert R. Natural hypometabolism during hibernation and daily torpor in mammals. *Respir Physiol Neurobiol* 141: 317–329, 2004.
- Heller HC, Ruby NF. Sleep and circadian rhythms in mammalian torpor. *Annu Rev Physiol* 66: 275–289, 2004.
- Jagoe RT, Lecker SH, Gomes M, Goldberg AL. Patterns of gene expression in atrophying skeletal muscles: response to food deprivation. *FASEB J* 16: 1697–1712, 2002.
- Knight JE, Narus EN, Martin SL, Jacobson A, Barnes BM, Boyer BB. mRNA stability and polysome loss in hibernating Arctic ground squirrels (*Spermophilus parryi*). *Mol Cell Biol* 20: 6374–6379, 2000.
- Kruman II, Ilyasova EN, Rudchenko SA, Khurkhulu ZS. The intestinal epithelial cells of ground squirrel (*Citellus undulatus*) accumulate at G₂ phase of the cell cycle throughout a bout of hibernation. *Comp Biochem Physiol A Physiol* 90: 233–236, 1988.
- Kuhn K, Baker SC, Chudin E, Lieu MH, Oeser S, Bennett H, Rigault P, Barker D, McDaniel TK, Chee MS. A novel, high-performance random array platform for quantitative gene expression profiling. *Genome Res* 14: 2347–2356, 2004.
- Liu B, Belk DD, Wang LC. Ca²⁺ uptake by cardiac sarcoplasmic reticulum at low temperature in rat and ground squirrel. *Am J Physiol Regul Integr Comp Physiol* 272: R1121–R1127, 1997.
- Lovegrove BG, Lawes MJ, Roxburgh L. Confirmation of pleiomorphic daily torpor in mammals: the round-eared elephant shrew *Macro-*

- celides proboscideus (Macroscelidea). *J Comp Physiol* 169: 453–460, 1999.
37. **Lust WD, Wheaton AB, Feussner G, Passonneau J.** Metabolism in the hamster brain hibernation and arousal. *Brain Res* 489: 12–20, 1989.
 38. **Martin S, Dahl T, Epperson LE.** Slow loss of protein integrity during torpor: a cause for arousal? In: *Life in the Cold: Evolution, Adaptation, Mechanisms, and Applications*, edited by Barnes BM, Carey HV. Fairbanks, AK: Institute of Arctic Biology, 2004.
 39. **McLeod CJ, Aziz A, Hoyt RF Jr, McCoy JP Jr, Sack MN.** Uncoupling proteins 2 and 3 function in concert to augment tolerance to cardiac ischemia. *J Biol Chem* 280: 33470–33476, 2005.
 40. **Mokuno K, Riku S, Sugimura K, Takahashi A, Kato K, Osugi S.** Serum creatine kinase isoenzymes in Duchenne muscular dystrophy determined by sensitive enzyme immunoassay methods. *Muscle Nerve* 10: 459–463, 1987.
 41. **Morano I.** Tuning the human heart molecular motors by myosin light chains. *J Mol Med* 77: 544–555, 1999.
 42. **Morano I, Adler K, Agostini B, Hasselbach W.** Expression of myosin heavy and light chains and phosphorylation of the phosphorylatable myosin light chain in the heart ventricle of the European hamster during hibernation and in summer. *J Muscle Res Cell Motil* 13: 64–70, 1992.
 43. **Morano I, Ritter O, Bonz A, Timek T, Vahl CF, Michel G.** Myosin light chain-actin interaction regulates cardiac contractility. *Circ Res* 76: 720–725, 1995.
 44. **O'Hara BF, Watson FL, Srere HK, Kumar H, Wiler SW, Welch SK, Bitting L, Heller HC, Kilduff TS.** Gene expression in the brain across the hibernation cycle. *J Neurosci* 19: 3781–3790, 1999.
 45. **Osborne PG, Hu Y, Covey DN, Barnes BM, Katz Z, Drew KL.** Determination of striatal extracellular gamma-aminobutyric acid in non-hibernating and hibernating arctic ground squirrels using quantitative microdialysis. *Brain Res* 839: 1–6, 1999.
 46. **Prendergast BJ, Freeman DA, Zucker I, Nelson RJ.** Periodic arousal from hibernation is necessary for initiation of immune responses in ground squirrels. *Am J Physiol Regul Integr Comp Physiol* 282: R744–R752, 2002.
 47. **Pruitt KD, Tatusova T, Maglott DR, NCBI.** Reference Sequence (RefSeq): a curated non-redundant sequence database of genomes, transcripts and proteins. *Nucleic Acids Res* 33: D501–D504, 2005.
 48. **Reppert SM, Weaver DR.** Molecular analysis of mammalian circadian rhythms. *Annu Rev Physiol* 63: 647–676, 2001.
 49. **Revel FG, Herwig A, Garidou ML, Dardente H, Menet JS, Masson-Pevet M, Simonneaux V, Saboureaux M, Pevet P.** The circadian clock stops ticking during deep hibernation in the European hamster. *Proc Natl Acad Sci USA* 104: 13816–13820, 2007.
 50. **Smit AF, Hubley R, Green P.** RepeatMasker Open-3.0 1996–2004 (<http://www.repeatmasker.org>).
 51. **Srere HK, Wang LCH, Martin SL.** Central role for differential gene expression in mammalian hibernation. *Proc Natl Acad Sci USA* 89: 7119–7123, 1992.
 52. **Teshima Y, Akao M, Jones SP, Marban E.** Uncoupling protein-2 overexpression inhibits mitochondrial death pathway in cardiomyocytes. *Circ Res* 93: 192–200, 2003.
 53. **Trachsel L, Edgar DM, Heller HC.** Are ground squirrels sleep deprived during hibernation? *Am J Physiol Regul Integr Comp Physiol* 260: R1123–R1129, 1991.
 54. **Van Gelder RN, von Zastrow ME, Yool A, Dement AC, Barchas JD, Eberwine EH.** Amplified RNA synthesized from limited quantities of heterogeneous cDNA. *Proc Natl Acad Sci USA* 87: 1663–1667, 1990.
 55. **Wada I, Rindress D, Cameron PH, Ou WJ, Doherty JJ II, Louvard D, Bell AW, Dignard D, Thomas DY, Bergeron JJ.** SSR alpha and associated calnexin are major calcium binding proteins of the endoplasmic reticulum membrane. *J Biol Chem* 266: 19599–19610, 1991.
 56. **Wang SQ, Lakatta EG, Cheng H, Zhou ZQ.** Adaptive mechanisms of intracellular calcium homeostasis in mammalian hibernators. *J Exp Biol* 205: 2957–2962, 2002.
 57. **Whitten BK, Klain G.** Protein metabolism in hepatic tissue of hibernating and arousing ground squirrel. *Am J Physiol* 214: 1360–1362, 1968.
 58. **Williams DR, Epperson LE, Li W, Hughes MA, Taylor R, Rogers J, Martin SL, Cossins AR, Gracey AY.** Seasonally hibernating phenotype assessed through transcript screening. *Physiol Genomics* 24: 13–22, 2005.
 59. **Yan J, Burman A, Nichols C, Alila L, Showe LC, Showe MK, Boyer BB, Barnes BM, Marr TG.** Detection of differential gene expression in brown adipose tissue of hibernating arctic ground squirrels with mouse microarrays. *Physiol Genomics* 25: 346–353, 2006.
 60. **Yatani A, Kim SJ, Kudej RK, Wang Q, Depre C, Irie K, Kranias EG, Vatner SF, Vatner DE.** Insights into cardioprotection obtained from study of cellular Ca²⁺ handling in myocardium of true hibernating mammals. *Am J Physiol Heart Circ Physiol* 286: H2219–H2228, 2004.
 61. **Yu XX, Lewin DA, Zhong A, Brush J, Schow PW, Sherwood SW, Pan G, Adams SH.** Overexpression of the human 2-oxoglutarate carrier lowers mitochondrial membrane potential in HEK-293 cells: contrast with the unique cold-induced mitochondrial carrier CGI-69. *Biochem J* 353: 369–375, 2001.
 62. **Zimmerman UJ, Wang P, Zhang X, Bogdanovich S, Forster R.** Anti-oxidative response of carbonic anhydrase III in skeletal muscle. *IUBMB Life* 56: 343–347, 2004.